ChemSearch Journal 8(2): 56 – 67, December, 2017
Publication of Chemical Society of Nigeria, Kano Chapter

Received: 12/10/2017 Accepted: 18/12/2017

Synthesis and Characterization of a Schiff Base Cobalt (III) Complex and Assessment of its Anti-Cancer Activity

Gwaram, N. S.
Department of Pure and Industrial Chemistry, Umaru Musa Yar'Adua University. P.M.B. 2211, Katsina, Nigeria.
Email: nura.suleiman@umyu.edu.ng

ABSTRACT

Cobalt (III) tris(azido)-2-Morpholino-*N*-(1-(2-pyridyl)ethylidene)ethanamine complex was synthesized, characterized and evaluated for *in vitro* anticancer activities. The chemical structure of the compound was assessed by elemental analysis, single crystal x-ray crystallography, FT-IR and UV-Visible spectroscopy. Schiff base molecule acts as tridentate ligand to form two five-membered chelate rings with the Co(III) ion. In the crystal structure three meridionally arranged nitrogen atoms from three azide ligands complete a distorted octahedral geometry around the metal center. The distortion from an ideal octahedron is evident from the cisoid [82.45(5)-96.03(5)^0] and transoid [168.62(5)-177.62(5)^0] angles. The azide groups are almost linear [175.65(15)-179.22(14)^0] whereas the Co-*N*-*N*-*N* linkages are significantly bent [114.33(9)-123.13(9)^0]. The novel cobalt(III) compound showed efficient anti-cancer activity against MCF-7 breast cancer cells. The compound was screened by MTT assay and was found to inhibit the growth of MCF-7 cells in a dose-dependent manner (IC50=2.80±0.02 µg/ml). The free ligand and free metal MTT assay showed no significant inhibition activities at a concentration even higher than the compound which confirmed that chelation of ligand with cobalt ion was significant for the activity of this novel compound. The cobalt compound activated caspase-3 via the intrinsic mitochondrial apoptotic pathway resulting in induces apoptosis on MCF-7 cell line.

Keywords: Co(III) compound; x-ray crystallography; MCF-7; Apoptosis; Anticancer activity

1NTRODUCTION

Transition metal complexes contribute largely to medicinal chemistry and are still the most widely used chemotherapeutic agents despite all limitations and side effects (Shazia *et. al.,* 2010, Powis 1991). Their pharmacological activities are attributed to the nature of the metal or ligand or both.

To design a metal complex for medical applications some important factors are considered such as maximum thermodynamic stability and large degree of selectivity. Metals from the first row transition play major roles in various biological activities and have been included in anticancer agents to exploit their various applications. This is because of the exceptionally wide range of reactivity available and have been particularly attractive (Petrovic 1996). They have been in use for medicinal purposes over a long period of time in a more or less empirical fashion (Thomson 2006), since the landmark discovery for the biological activity of cisplatin the potential of metal-based anticancer agents has been realized and explored (Shahabadi 2010). This has driven inorganic and organometallic chemists to look for new metal compounds with good activities, preferably against tumors that are responsible for high cancer mortality (El-sherif and Eldebss 2011). Therefore research has been extended to practically all metals, among which the Schiff base compounds of cobalt, copper, nickel, manganese, zinc, palladium, magnesium and gold and most transition metal compounds show most promising results (Bagihalli *et. al.,* 2008, Creaven *et. al.,* 2010, Bernadette *et. al.,* 2010, Garoufis *et. al.,* 2009, Wang *et. al.,* 2005). Transition metal compounds offer a great diversity in their action. For example they have been reported to have anti-cancer properties (Qiao *et. al.,* 2011, Etcheverry *et. al.,* 2012, Raman *et. al.,* 2010, Shakir *et. al.,* 2011), and have also been used as anti-inflammatory and anti-arthritic agents with DNA binding and DNA cleavage activities (El-sherif and Eldebss 2011).

Morpholine derived compounds are completely stable in biological systems, allowing rigorous long-term applications as they constitute a radical re-design of DNA. When the 5-membered deoxyribose rings of DNA are replaced by 6-membered morpholine rings; and the negatively charged inter-subunit linkages of DNA are replaced by non-ionic inter-subunit linkages (Summerton 2007). These changes and consequence of their novel backbone structure provide decisive advantages over the more conventional oligo types used for modulating gene expression.

Cobalt is a key constituent of cobalamin and essential to all animals, including humans. Cobalamin which is also known as vitamin B_{12}, is the primary biological reservoir of cobalt as an "ultratrace" element. It is widely distributed in the biological systems such as cells and body, and thus the interaction of DNA with cobalt compound has attracted much attention (Hisashi 2003). The binding properties of cobalt with calf thymus DNA were studied by several methods, and the experimental results showed that the size and shape of the intercalated ligand had an important effect on the binding affinity of the compounds with DNA (Vaidyanathan 2003). Hisaeda and co-workers (2003) discovered a new water-soluble dicobalt compound having two cobalt-carbon bonds and reported that this dicobalt compound showed higher ability for DNA cleavage in comparison with the corresponding monocobalt compound (Zhaang 2003). The interaction of DNA with cobalt(II) tridentate compound, and the photocleavage studies showed that the cobalt(II) compound increased to nicking of DNA in the presence of plasmid DNA (Jiao 2005).

In this study, we examined the potential anti-cancer of cobalt(III) compound of *N,N',N"* donor Schiff base ligand from the reaction of 4-(2-aminoethyl)morpholine and 2-acetylpyridine in presence azide (N_3^- ion) for apoptotic application on human breast cancer MCF-7 cell line.

MATERIALS AND METHODS

Reagents and instrumentation

All chemicals were of analytical grades and used without any further purification. Cobalt(II) acetate, sodium azide, 4-(2-aminoethyl)morpholine and 2-acetylpyridine were purchased from Aldrich–Sigma Company. Ethanol was distilled prior to use. Melting points were determined using an MEL-TEMP II melting point instrument. Microanalyses were carried out on a Perkin-Elmer 2400 elemental analyzer. 1H-NMR and 13C-NMR spectra were determined with a JEOL Lambda 400 MHz FT-NMR (1H: 400 MHz and 13C: 100.4 MHz) spectrometer. Chemical shifts are given in δ values (ppm) using TMS as the internal standard.

Cell Lines

Human breast cancer MCF-7 cell line was obtained from the American Type Culture Collection ATCC, USA.

Synthesis of Cobalt(III)Complex

A mixture of 2-acetylpyridine (0.20 g, 1.65 mmol) and 4-(2-aminoethyl)morpholine (0.21 g, 1.65 mmol) in ethanol (20 ml) was refluxed for 2 hr followed by addition of a solution of cobalt(II) acetate tetrahydrate (0.41 g, 1.65 mmol) and sodium azide(0.22 g, 3.30 mmol) in a minimum amount of water. The resulting solution was refluxed for 30 mins, and then left at room temperature two days. The crystals of the title compound (Figure 1) were obtained in a two days; the resulting crystal was filtered off, washed with cold ethanol and dried over silica gel. Brown solid, 95% yield, m.p. >400 ºC. Analytical calculated for $C_{13}H_{19}CoN_{12}O$ (418.3); Theory: C, 41.85; H, 5.67; N, 28.16. Found: C, 40.65; H, 5.60; N, 28.32. IR: ATR ν_{max}/cm^{-1} 3277.80 (CH aromatic), 2877.16, 2944.00 (CH aliphatic), 1992.40 (N=N=N azide), 1646.00 (C=N Schiff), 1428.41 (C-C), 1112.30 (C-N), 571.87 (M-N). UV-Vis: λ_{max}/nm DMSO 778.00 (d→d*), 596.00 (LMCT); 403, 343 (n→π*); 266 (π→π*).

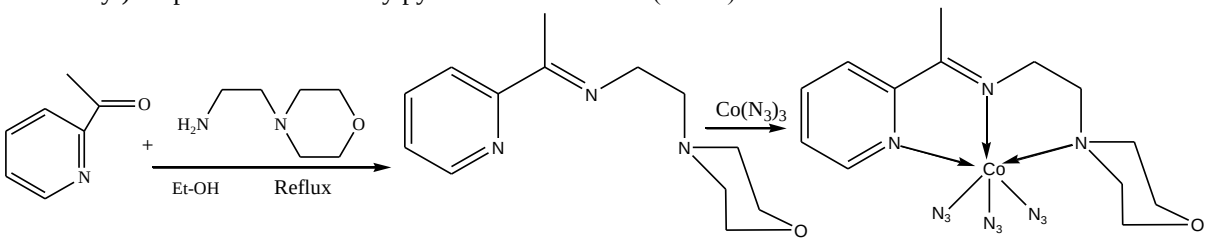

Fig. 1: Proposed synthesis scheme for $[Co(N_3)_3(C_{13}H_{19}N_3O)]$

Single Crystal X-Ray Diffraction

Diffraction data were measured using a Bruker SMART Apex II CCD area-detector diffractometer (graphite-monochromated Mo K radiation, = 0.71073 Å). The orientation matrix, unit cell refinement and data reduction were all handled by the Apex2 software (SAINT integration, SADABS absorption correction) (Inc 2007). The structure was solved using direct method in the program SHELXS-97 (Sheldrickn20008) and was refined by the full matrix least-squares method on *F2* with SHELXL-97. All the non-hydrogen atoms were refined anisotropically and all the hydrogen atoms were placed at calculated positions and refined isotropically. Drawing of the molecule was produced with XSEED (Barbour 2001). Crystal data and refinement are summarized in Table 1.

Table 1: Crystal data and refinement parameters of $[Co(C_{13}H_{19}N_3O)(N_3)_3]$.

Empirical formula	$C_{13}\ H_{19}\ Co\ N_{12}\ O$
Crystal system	Monoclinic
Space group	*P 21/c*
Unit cell dimensions	
a (Å)	10.0164(2)
b (Å)	12.6221(3)
c (Å)	13.7134(3)
β (°)	91.1770(9)
Volume (Å^3)	1733.39(7)
Z	4
Density (calculated) (g cm^{-3})	1.603
Crystal size (mm^3)	0.27 x 0.21 x 0.18
θ range for data collection (°)	2.03 to 27.00
Reflections collected	15495
Independent reflections	3783 [R_{int} = 0.0199]
Completeness	To *θ* = 27° : 99.9 %
Data / restraints / parameters	3783 / 2 / 245
Goodness-of-fit on F^2	1.103
Final *R* indices [$I>2\sigma$ (I)]	R_1 = 0.0223, wR_2 = 0.0540
R indices (all data)	R_1 = 0.0253, wR_2 = 0.0553

Cytotoxicity evaluation

MTT - Culture of cells and cytotoxicity assay

Human breast cancer MCF-7 cell line was seeded into 96-well plate at an initial cell density of approximately 5x10^5 cells per well. After 24 hrs incubation for cell attachment and growth, the medium was removed and replaced with fresh medium containing different concentrations of the compounds. The compound added was first dissolved in DMSO at the 1.5, 3 and 4.5 µg/ml required concentrations. Subsequent six desirable concentrations were prepared using growth medium. Control wells received only DMSO. Each concentration of the compound was assayed in six replicates within 48 hrs incubation period. Again, the medium was removed and cell viability was determined after further 4 hrs with 5 mg per ml of MTT [3-(4,5-dimethylthiazol-2-yl)-2,5-diphenyltetrazolium]bromide. DMSO was then added per well and the dissolving formazan precipitate was read by using elisa plate reader, Dynatech MR5000, at 570 nm and comparison was made with positive control tamoxifen.

Determination of caspase-3 activity by absorption spectroscopy

The measurement of caspase-3 activity was performed by caspase colormetric protease assay kit, according to manufacturer's instructions (Jun 2009). The absorbance of each sample at 405 nm was read by a Bio-Rad 680 microplate reader.

Statistical Analysis

All data were expressed as Mean ± SD (standard deviation) by an assessment of differences using SPSS 16.0 software.

Molecular Modeling Evaluations

The coordinates for the enzyme were those deposited in the Protein Data Bank for caspase 3 (1PAU) after eliminating the inhibitor (AC-DEVD-CHO) and water molecules. The missing residues were built and polar hydrogen atoms were added using Discovery Studio 3.0 (Accelrys, Inc., San Diego, CA, USA). By default, solvation parameters and Kollman charges were assigned to all atoms of the enzyme using AutoDock Tools v.1.4. The 3D structures of the compounds were optimized according to the standard protocol in Discovery Studio 3.0. For docking studies, the latest version of AutoDock v.4.0 (Morris 1998) was chosen because its algorithm allows full flexibility of small compounds. It has also been shown to successfully reproduce many crystal structure complexes and includes an empirical binding free energy evaluation. Docking of compounds to caspase 3 was carried out using the hybrid Lamarckian Genetic Algorithm. A grid box with the size of 150 x 140 x 110 grid box, and grid spacing of 0.375 Å was built to span the entire protein structure, in vacuo. The maximum number of energy evaluations was set to 25,000,000. Blind docking was used to predict structural features of compound binding. Resulting docked orientations within a root-mean square deviation of 1.5 Å were clustered. The lowest energy cluster reported by AutoDock for the compound was used for further analysis. All other parameters were maintained at their default settings. The structure of the complex obtained was visualized and analyzed using Discovery Studio Visualizer 3.0 and Ligplot 1.0 (Wallace 1995) to identify specific interactions between the atoms of the compound and the enzyme.

RESULTS AND DISCUSSION

The *N,N',N"* donor Schiff base was synthesized from the reaction of 4-(2-aminoethyl)morpholine, with 2-acetylpyridine in presence of sodium azide N_3^- ion coordinates with cobalt(II) ion giving rise to coordination compound of cobalt(III). The characteristic IR stretching frequency of the metal compound along with the proposed assignments are summarized in experimental part. The IR spectra of all the compound possess very strong characteristic absorption bands in the region of 1649-1661cm^{-1} which is attributed to the C=N stretching vibration of the Schiff base imino functional group, a similar has been reported. (Raman and Sudharsan 2011, Khan *et. al.*, 2011, Nakamoto 1978, Laskar 2001). A chemical shift was observed at a region of 2070cm^{-1} and 2043cm^{-1} which is attributed to cobalt to azide metal bond (Bhowmik *et. al.*, 2010). The spectra for the compound showed M–N bands at a lower wavelength in the range of 477-575 cm^{-1} (Salga 2012, Abdelaziz 2010).

The electronic spectra for all the compounds were obtained in DMSO solvent and showed absorption band in three distinct regions. The first region ranging from 224 to approximately 280 nm, is characteristic for the electronic inter-ligand $\pi \rightarrow \pi^*$ transitions (Mustapha 2009), while the second characteristic wavelength in the region of 281 nm to approximately 409 nm is the second inter ligand $n \rightarrow \pi$ transition (Yusnita 2009). The third distinct region ranging from 492 nm to approximately 606 nm is the characteristic for the ligand to metal charge transfer (LMCT) from the nitrogen atom to the transition metal centre (Yusnita 2009). The last distinct region ranging from 650 nm to approximately 750 nm is the characteristic for the inter metal $d \rightarrow d^*$ transition (Yusnita 2009).

The molecular structure of Co(III) compound is depicted in (Figure 2) and selected bond lengths and angles are listed in Table 2. In the compound, the Schiff base molecule acts as an *N,N',N"*-tridentate ligand to form two five-membered chelate rings with the Co(III) atom. Three meridionally arranged nitrogen atoms from three azide ligands complete a distorted octahedral geometry around the metal center. The distortion from an ideal octahedron is evident from the cisoid [82.45(5)-96.03(5)^0] and transoid [168.62(5)-177.62(5)^0] angles (Table 2). The azide groups are almost linear [175.65(15)-179.22(14)^0] whereas the Co-*N*-*N*-*N* linkages are significantly bent [114.33(9)-123.13(9)^0]. The Co-N bond lengths are similar to those observed in a similar structure (Rahaman 2005).

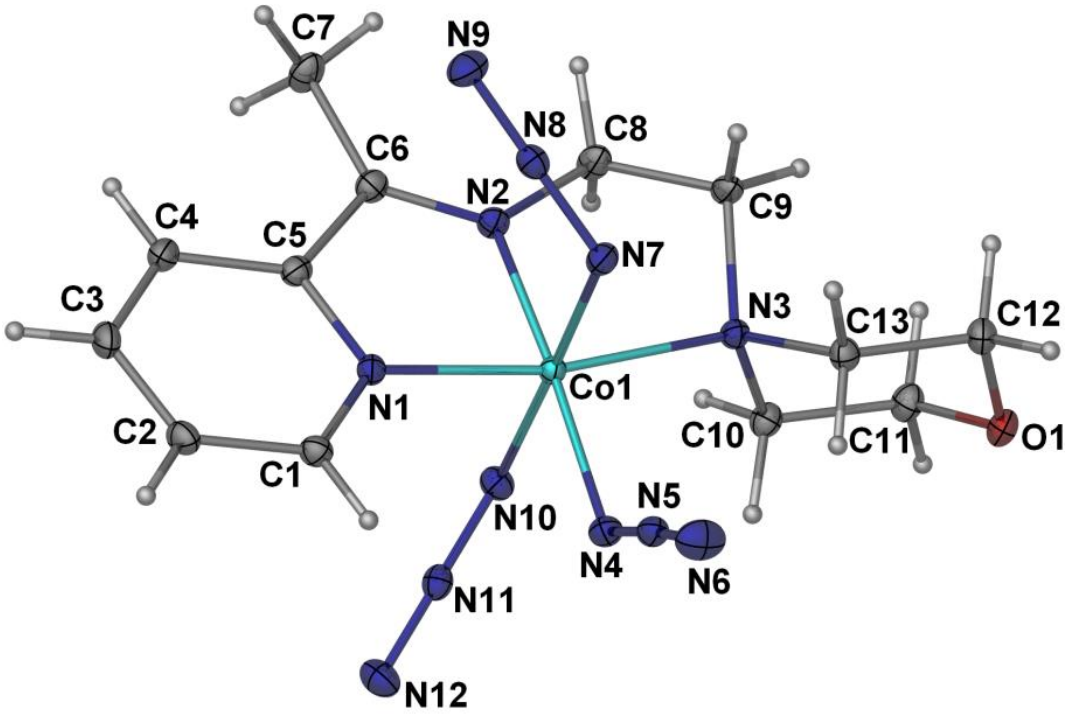

Fig. 2: The molecular structure of $[Co(N_3)_3(C_{13}H_{19}N_3O)]$ (30% probability ellipsoids). Hydrogen atoms are drawn as spheres of arbitrary radius.

Table 2: Selected bond lengths [Å] and bond angles [°] of $[Co(C_{13}H_{19}N_3O)(N_3)_3]$.

Bond lengths			
Co(1)-N(2)	1.8777(11)	N(4)-N(5)	1.2018(16)
Co(1)-N(1)	1.9257(11)	N(5)-N(6)	1.1514(17)
Co(1)-N(4)	1.9407(11)	N(7)-N(8)	1.2104(16)
Co(1)-N(10)	1.9699(12)	N(8)-N(9)	1.1545(17)
Co(1)-N(7)	1.9777(12)	N(10)-N(11)	1.2079(16)
Co(1)-N(3)	2.0334(11)	N(11)-N(12)	1.1552(17)
Bond angles			
N(2)-Co(1)-N(1)	82.45(5)	N(1)-Co(1)-N(3)	168.62(5)
N(2)-Co(1)-N(4)	175.54(5)	N(4)-Co(1)-N(3)	95.18(5)
N(1)-Co(1)-N(4)	96.03(5)	N(10)-Co(1)-N(3)	93.39(5)
N(2)-Co(1)-N(10)	88.04(5)	N(7)-Co(1)-N(3)	88.92(5)
N(1)-Co(1)-N(10)	89.02(5)	N(6)-N(5)-N(4)	175.65(15)
N(4)-Co(1)-N(10)	87.74(5)	N(9)-N(8)-N(7)	179.22(14)
N(2)-Co(1)-N(7)	92.68(5)	N(12)-N(11)-N(10)	177.56(14)
N(1)-Co(1)-N(7)	88.83(5)	N(5)-N(4)-Co(1)	123.13(9)
N(4)-Co(1)-N(7)	91.48(5)	N(8)-N(7)-Co(1)	114.85(9)
N(10)-Co(1)-N(7)	177.62(5)	N(11)-N(10)-Co(1)	114.33(9)
N(2)-Co(1)-N(3)	86.52(5)		

The Co(II) ion with its d^7 configuration commonly exhibits octahedral geometries (Bagihalli 2008). The d-d peaks on the spectrum (Figure 3) are transitions for the d^6 cobalt(III) complex in $[Co(LMA)(N_3)_3]$ bands at 240, 395, 416, 596 nm attributable to 1A1g→3A1g; 1Aig→3T2g and 1Aig→5T2g Judging by the Tanabe-Sugano diagram for d^6 complexes, the ground state 5D would be split into a $^5T_{2g}$ and a ^5E_g. The stronger of the two peaks is most likely the transition between these two states. The weaker peak may be a spin-forbidden transition, which cannot be accurately predicted. The complex is most likely weak field, with four unpaired electrons.

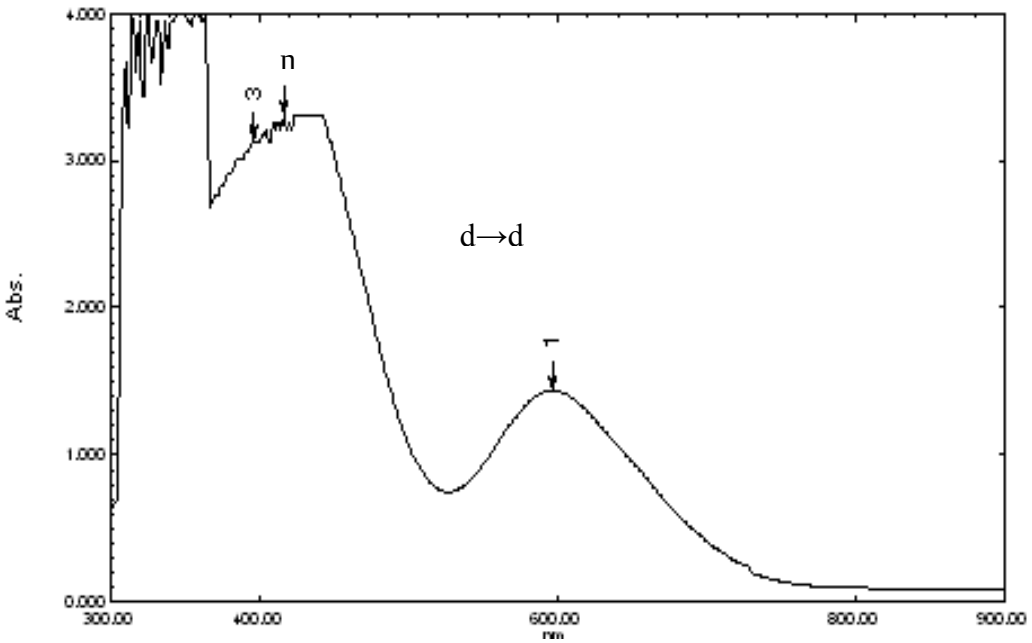

Fig. 3: Electronic spectra for $[Co(N_3)_3(C_{13}H_{19}N_3O)]$

MTT assay was used to determine the cobalt compound cytotoxicity against human breast cancer MCF-7cell line. This assay served as an index used to determine cytotoxicity of cobalt compound to stimulate or inhibit cell viability and growth. This is by detecting the reduction of tetrazolium salt to blue formazan by mitochondrial enzyme activity of succinate dehydrogenase in living cells. MCF-7 cells were treated with different concentrations of the cobalt compound for 48 h, and the cells viability were measured by MTT assay. The cobalt(III) compound was found to inhibit the growth of MCF-7 cells in a dose-dependent manner (IC50=2.80±0.02 µg/ml). The

MTT assay of free ligand and free metal showed no significant inhibition activities at a concentration even higher than the chelation of ligand with cobalt ion was observed (Table 3).

Clonogenic assay is used for studying the effectiveness of specific agents on the survival and proliferation of cells. In this study the effectiveness for the cytotoxicity of cobalt(III) compound to inhibit growth of MCF-7 cells was determined; Cells were trypsinised and counted to a ratio of 5×10^3 cells per plate. The colony-forming cells number using the cobalt compound at concentration of 2.80, 3.72 and 4.53 µg/ml was reduced compared to the untreated MCF-7 as a control. No colony observed at the concentration of higher than 8.56 µg/ml, indicating the cobalt(III) compound showed toxicity and inhibited the proliferation of MCF-7 cell. Toxicity of compound was further supported by clonogenic efficiency (CE) which is the number of colonies divided by the number of cells added to each plate. This result is consistent with the result of MTT assay (IC_{50}) (Table 3).

Table 3 Comparison of clonogenic efficiency (CE) at different concentrations with untreated cell line (as control) on MCF-7 cell line. The results are expressed as the Mean±SD (n=3).

	Different concentrations of compound (µg/ml)	**Apoptotic colonies (%)**	**Number of viable colonies**	**CE***
Co(III)	**2.80±0.02** (IC50)	50.60	560	0.112
Co(III)	3.72±0.05	58.30	480	0.096
Co(III)	4.53±0.03	68.73	200	0.04
Co(III)	8.56±0.02	100	No colony	0
Co(III)	12.45±0.03	100	No colony	0
Control	-	0	1150	0.23

*CE: Clonogenic efficiency.

To further confirmation of the cobalt compound induced apoptosis in MCF-7 cells, caspase activity and potential molecular mechanisms involved were measured, colorimetric was upon treatment with 1.5, 3 and 4.5 µg/ml cobalt compound for 48 h. The activity of caspase-3 increased remarkably in MCF-7 cells after administration of cobalt compound via the intrinsic mitochondrial apoptotic pathway in caspase-3 activity, which confirmed the apoptosis of MCF-7 cells induced by cobalt compound (Figure 4).

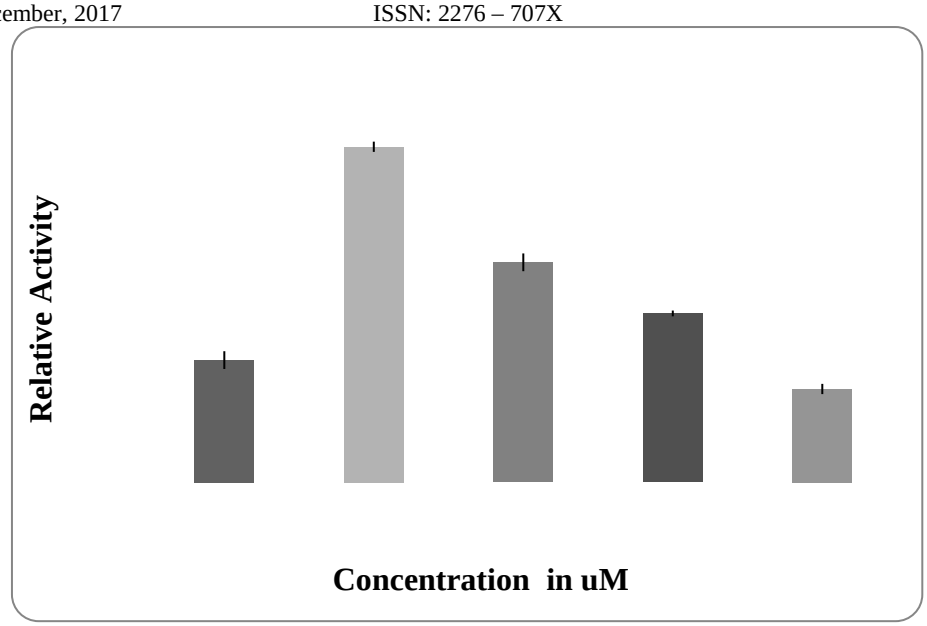

Fig. 4: The activities of caspase-3 after treatment with various concentrations of $[Co(N_3)_3(C_{13}H_{19}N_3O)]$ compound for 48 h. The activities of caspase-3 were expressed relative to the untreated control. The results are expressed as the Mean ± SD (n=3)

Caspase 3 (pdb id: 1PAU) is a member of the cysteine-aspartic acid protease (caspase) family (Alnemri 1996). Sequential activation of caspase 3 plays a central role in the execution-phase of cell apoptosis. The catalytic site of caspase-3 involves the sulfohydryl group of Cys-285 and the imidazole ring of His-237. His-237 stabilizes the carbonyl group of the key aspartate residue, while Cys-285 attacks to ultimately cleave the peptide bond. Cys-285 and Gly-238 also function to stabilize the tetrahedral transition state of the substrate-enzyme complex through hydrogen bonding (Lavrik 2005).

Fig. 5: (a)

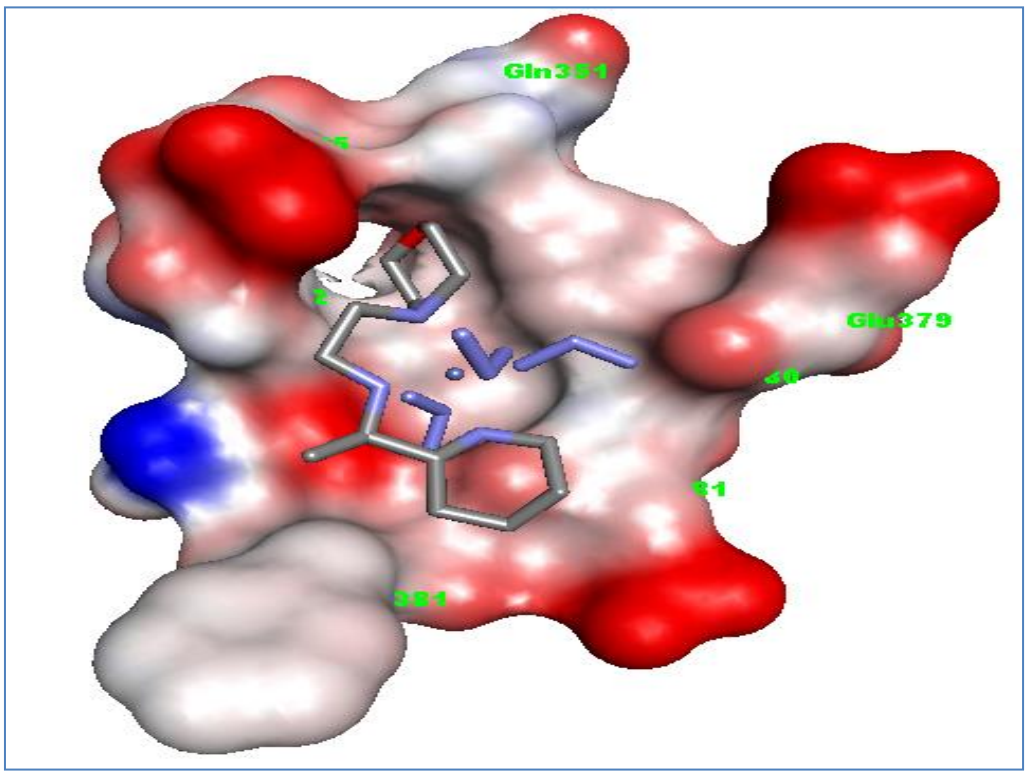

(**b**)

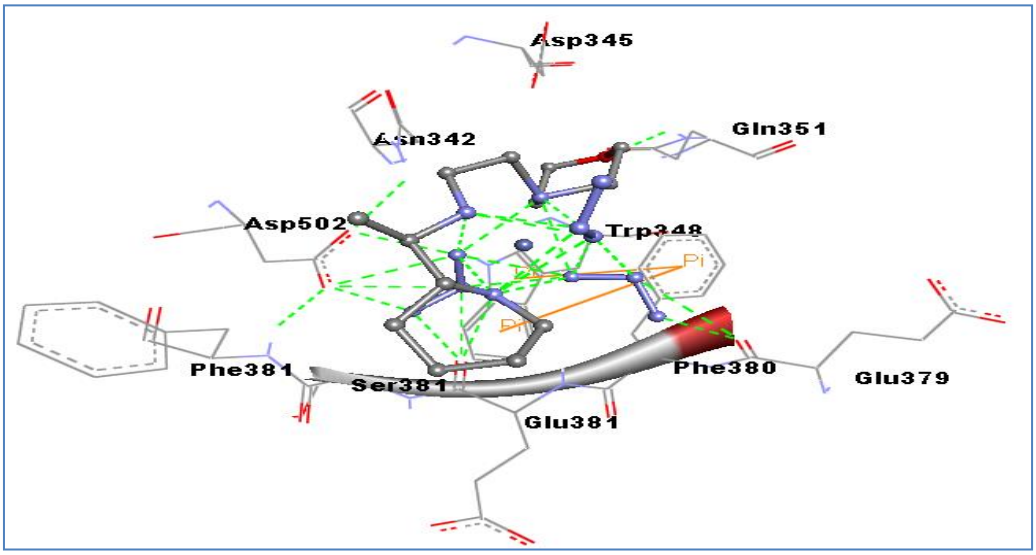

(**c**)

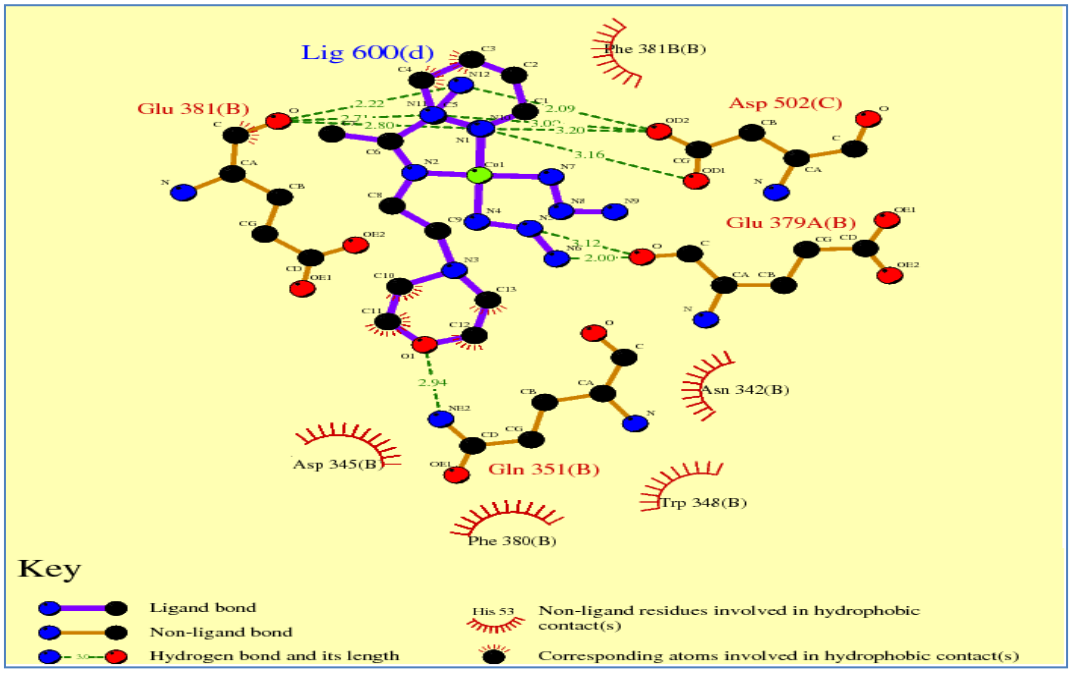

Fig. 5(a) Representations of the molecular model of the complex formed between $[Co(N_3)_3(C_{13}H_{19}N_3O)]$ and Caspase 3 (1PAU). (**b**) 3D representation of the ligand-enzyme binding interactions, cobalt(III) is represented as a dark grey sticks and hydrogen bonds as green dashed lines; (**c**) 2D schematic representation of the hydrogen bonding and hydrophobic interactions.

From the molecular docking simulation carried out, it can be seen that the residues involved in the interactions with the cobalt(III) compound are Asn 342, Asp 345, Asp 502, Gln 351, Glu 379, Glu 380, Glu 381, Phe 380, Phe 381, Ser 381, and Trp 348 (Figure 5 a-c). The complex formed between cobalt(III) compound and caspase 3 showed that the ligand does not bind to the active-site gorge. and due to the fact that the caspase-3 zymogen has virtually no activity until it is cleaved by an initiator caspase after apoptotic signaling events have occurred (WALTERS 2009) therefore, the introduction of cobalt(III) compound can activate caspase 3 initiator, into cells targeted for apoptosis (Gallaher 2001, Katunuma 2001). This extrinsic

activation then triggers the hallmark caspase cascade characteristic of the apoptotic pathway, in which caspase-3 plays a dominant role (Perry 1997). In intrinsic activation, cytochrome c from the mitochondria works in combination with ATP to process procaspase-3 (Katunuma 2001, Porter 1999, Li 2004). This is evident that this compound activated caspase-3 in vitro, but other regulatory proteins are necessary in vivo (Li 2004).

A closer inspection of the interactions (Fig. 5b) showed the presence of hydrogen bond between the oxygen attached to the morpholine group with Gln 351 (B), π-π and cation-π stacking involving between nitrogen atoms from the azide groups and Glu 379(A), Glu 381(B) and Asp 502(C). Furthermore, hydrophobic interactions between ligand and caspase 3 residues [Phe 381 B(B), Asp 345 (B), Phe380 (B), Trp 348 (B) and Asn 342(B)] was observed which enables the morpholine oxygen to form a hydrogen bond with Gln 351(B) and azide groups to form a cluster of networking hydrogen bonds with Asp 502(C) and Glu 381(B).

The studies of Reactive oxygen species ROS effects on biological systems, underlying mechanisms and therapeutic implications largely depend on proper experimental models (Weiqin 2007). Figure 8 shows the ROS values for the $[Co(N_3)_3(C_{13}H_{19}N_3O)]$ compound in two different concentrations (1.5ug/ml = 704 and 2ug/ml = 793.5) higher than the control (Figure 6). Increased generation of reactive oxygen species (ROS) has been observed in cancer, degenerative diseases, and other pathological conditions (Weiqin 2007). Evidence exists that the role of ROS in cancer is not limited to the generally accepted genotoxicity and mutagenic effects that initiate cancer. As signal transduction messengers, ROS may promote either proliferation or death of cancer cells, depending on the actual intracellular and exogenous conditions (Gina *et. al.*, 2009). ROS were shown to modulate growth signals and to activate gene expression, leading to sustained proliferation of cancer cells (Filomeno *et. al.*, 2005).

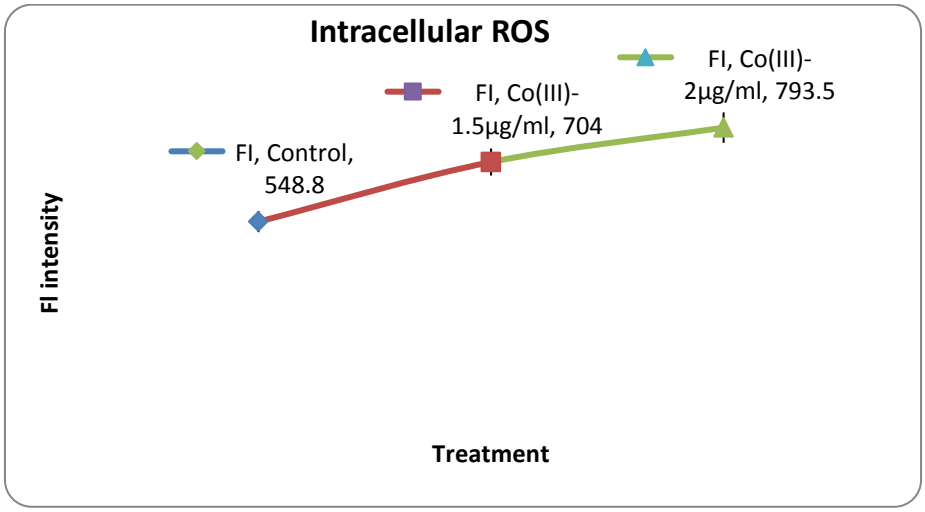

Fig. 6: ROS values for the $[Co(N_3)_3(C_{13}H_{19}N_3O)]$ compound in two different concentrations

CONCLUSIONS

In this study, we have studied interaction of $[Co(N_3)_3(C_{13}H_{19}N_3O)]$ Schiff base compound with nucleic acids and analyzed its biochemical effect on human breast cell line. X-ray crystal structures of this compound exhibits $[Co(N_3)_3(C_{13}H_{19}N_3O)]$ in a distorted octahedral geometry around the metal center with the Schiff base ligand having an *N, N, N* chelating motif. In cytotoxicity research, the compound showed high *in vitro* cytotoxic properties with significant growth inhibition activity against MCF-7cell line. The compound could induce apoptosis by alteration of nucleus morphology and mitochondrial membrane changes, inhibition of colony formation, DNA fragmentation and cytopathologic effects on the MCF-7 cells. The potential mechanism for apoptosis induction was attributed to triggering the intrinsic mitochondrial apoptotic pathway owing to activation of caspase-3. The data from our present study suggested that the efficient capability of the compound to inhibit growth activities as anti-cancer compound against human breast MCF-7cell line in which deserves further investigation on other human cell lines as new antitumor drug.

ACKNOWLEDGMENTS

The authors would like to thank the Department of Chemistry, Faculty of Science, University of Malaya for the provision of laboratory facilities.

SUPPLEMENTARY DATA

CCDC 861277 contains the supplementary crystallographic data for compound. This data can be obtained free of charge via http://www.ccdc.cam.ac.uk/ conts/retrieving.html, or from the Cambridge Crystallographic Data Centre, 12 Union Road, Cambridge CB2 1EZ, UK; fax: (+44) 1223-336-033; or e-mail: deposit@ccdc.cam.ac.uk.

REFERENCES

Abdel Aziz AA (2010). Synthesis, spectroscopic characterization, thermal studies, catalytic epoxidation and biological activity of chromium and molybdenum hexacarbonyl bound to a novel N2O2 Schiff base. *Journal of Molecular Structure* 979: 77-85.

Alnemri ES, Livingston DJ, Nicholson DW, Salvesen G, Thornberry NA, Wong WW and J. Y (1996). Human ICE/CED-3 protease nomenclature. *cell* 87: 171.

Bagihalli GB, Avaji PG, Patil SA and Badami PS (2008). Synthesis, spectral characterization, in vitro antibacterial, antifungal and cytotoxic activities of Co(II), Ni(II) and Cu(II) complexes with 1,2,4-triazole Schiff bases. *European Journal of Medicinal Chemistry* 43: 2639-2649.

Barbour LJ (2001) A Software Tool for Supramolecular Crystallography Journal of Supramolecular Chemistry 1: 189-191.

Bernadette SC, Brian D, Denise AE, Kevin K, Georgina R, Venkat Reddy T and Maureen W (2010). Anticancer and antifungal activity of copper(II) complexes of quinolin-2(1H)-one-derived Schiff bases. *Inorganica Chim Acta* 363: 4048-4058.

Bhowmik P, Chattopadhyay S, Drew MGB, Diaz C and Ghosh A (2010). Synthesis, structure and magnetic properties of mono- and di-nuclear nickel(II) thiocyanate complexes with tridentate N3 donor Schiff bases. *Polyhedron* 29: 2637-2642.

Creaven BS, Devereux M, Foltyn A, McClean S, Rosair G, Thangella VR and Walsh M (2010). Quinolin-2(1H)-one-triazole derived Schiff bases and their Cu(II) and Zn(II) complexes: Possible new therapeutic agents. *Polyhedron* 29: 813-822.

El-Sherif AA and Eldebss TMA (2011). Synthesis, spectral characterization, solution equilibria, in vitro antibacterial and cytotoxic activities of Cu(II), Ni(II), Mn(II), Co(II) and Zn(II) complexes with Schiff base derived from 5-bromosalicylaldehyde and 2-aminomethylthiophene. *Spectrochimica Acta Part A: Molecular and Biomolecular Spectroscopy* 79: 1803-1814.

Etcheverry S.B., Di Virgilio A.L., Nascimento O.R. and Williams P.A.M (2012). Dinuclear copper(II) compounds with valsartan. Synthesis, characterization and cytotoxicity. Journal of *Inorganic Biochemistry* 107: 25–33.

Filomeno G, Rotilio G and MR. C (2005). Disulfide relays and phosphorylative cascades: partners in redox-mediated signaling patways. Cell Death and Differenciation 12: 1555-63.

Gallaher BW, Hille R, Raile K and W. K (2001). Apoptosis: live or die--hard work either way! *Hormone and Metabolic Research* 33: 511-519.

Garoufis A, Hadjikakou SK and Hadjiliadis N (2009). Palladium coordination compounds as anti-viral, anti-fungal, anti-microbial and anti-tumor agents. *Coordination Chemistry Reviews* 253: 1384-1397.

Gina Manda, Nechifor MT and Teodora-Monica Neagu (2009). Reactive Oxygen Species, Cancer and Anti-Cancer Therapies. *Current Chemical Biology* 3: 342-366.

Hisashi S. Takeshi K. Takashi M., Sato H and Hisaeda Y. (2003). Syntheses of new water-soluble dicobalt complexes having two cobalt-carbon bonds and their ability for DNA cleavage. *Tetrahedron Letters* 44.

Inc. BA (2007). Analytical X-ray Instruments Inc. In: Bruker (ed) Bruker AXS, Madison, Wisconsin, USA.

Jiao K, Wang QX, Sun W and Jian FF (2005). Synthesis, characterization and DNA-binding properties of a new cobalt(II) complex: Co(bbt)2Cl2. *Journal of Inorganic Biochemistry* 99: 1369-1375.

Jung Y and SJ. L (2007). Direct cellular responses to platinum-induced DNA damage. *Chemical reviews* 107: 1387–1407.

Jun Tan, Bochu Wang and Zhu L (2009). DNA binding and oxidative DNA damage induced by a quercetin copper(II) complex: potential mechanism of its antitumor properties. Journal of Biological Inorganic Chemistry 5: 727-739.

Katunuma N, Matsui A, Le QT, Utsumi K, Salvesen G and A. O (2001). Novel procaspase-3 activating cascade mediated by lysoapoptases and its biological significances in apoptosis. *Advances in Enzyme Regulation* 41: 237-50.

Kerr JFR HB (1991). Definition and incidence of apoptosis: An historical perspective. Cold Spring Harbor Laboratory Press, Cold Spring Harbor, New York.

Khan N-uH, Pandya N, Prathap KJ, Kureshy RI, Abdi SHR, Mishra S and Bajaj HC (2011).

Chiral discrimination asserted by enantiomers of Ni (II), Cu (II) and Zn (II) Schiff base complexes in DNA binding, antioxidant and antibacterial activities. *Spectrochimica Acta Part A: Molecular and Biomolecular Spectroscopy* 81: 199-208.

Laskar IR, Maji TK, Das D, Lu TH, Wong WT, Okamoto Ki and Ray Chaudhuri N (2001). Syntheses, characterisation and solid state thermal studies of 1-(2-aminoethyl)piperidine (L), 1-(2-aminoethyl)pyrrolidine (L') and 4-(2-aminoethyl)morpholine (L") complexes of nickel(II): X-ray single crystal structure analyses of trans-[NiL2(CH3CN)2](ClO4)2, trans-[NiL2(NCS)2] and trans-[NiL"2(NCS)2]. *Polyhedron* 20: 2073-2082.

Lavrik IN, Golks A and PH. K (2005). Caspases: pharmacological manipulation of cell death. *The Journal of Clinical Investigation* 115: 2665-2672.

Li P, Nijhawan D and X. W (2004). Mitochondrial activation of apoptosis. *Cell*. 116: S57-9.

Morris GM, Goodsell DS, Halliday RS, Huey R, Hart WE, Belew RK and Olson AJ (1998). Automated docking using a Lamarckian genetic algorithm and empirical binding free energy function. *Journal od Computational Chemistry* 19: 1639–1662.

Mustafa IM, Hapipah MA, Abdulla MA and Ward TR (2009). Synthesis, structural characterization, and anti-ulcerogenic activity of schiff base ligands derived from tryptamine and 5-chloro, 5-nitro, 3,5-ditertiarybutyl salicylaldehyde and their nickel(II), copper(II), and zinc(II) complexes. *Polyhedron* 28: 3993-3998.

Nakamoto K (1978). Infrared and Raman Spectra of Inorganic and Coordination Compounds. John Wiley & Sons Inc, Atlanta, GA, U.S.A.

Perry DK, Smyth MJ, Stennicke HR, Salvesen GS, Duriez P, Poirier GG and YA. H (1997). Zinc is a potent inhibitor of the apoptotic protease, caspase-3. A novel target for zinc in the inhibition of apoptosis. *The Journal of Biological Chemistry* 272: 18530-3.

Petrovic N., Comi A. and Ettinger M.J (1996). Identification of an Apo-Superoxide Dismutase (Cu,Zn) Pool in Human Lymphoblasts. Journal of Biological Chemistry 271: 28331–28334.

Porter AG and RU. J (1999). Emerging roles of caspase-3 in apoptosis. *Cell Death & Differentiation* 6: 99-104.

Powis G. and Hacker M.P (1991). The Toxicity of Anticancer Drugs. *Pergamon Press*, New York, USA.

Qiao X, Ma Z-Y, Xie C-Z, Xue F, Zhang Y-W, Xu J-Y, Qiang Z-Y, Lou J-S, Chen G-J and Yan S-P (2011). Study on potential antitumor mechanism of a novel Schiff Base copper(II) complex: Synthesis, crystal structure, DNA binding, cytotoxicity and apoptosis induction activity. *Journal of Inorganic Biochemistry* 105: 728-737.

Rahaman SH, Chowdhury H, Bose D, Ghosh R, Hung C-H and Ghosh BK (2005). Synthesis, structure and properties of mononuclear cobalt(II) and cobalt(III) pseudohalide complexes containing N-donor Schiff bases: Synthetic control of metal oxidation levels. Polyhedron 24: 1755-1763.

Raman N, Jeyamurugan R, Senthilkumar R, Rajkapoor B and Franzblau SG (2010). In vivo and in vitro evaluation of highly specific thiolate carrier group copper(II) and zinc(II) complexes on Ehrlich ascites carcinoma tumor model. *European Journal of Medicinal Chemistry* 45: 5438-5451.

Raman N, Selvan A and Sudharsan S (2011). Metallation of ethylenediamine based Schiff base with biologically active Cu(II), Ni(II) and Zn(II) ions: Synthesis, spectroscopic characterization, electrochemical behaviour, DNA binding, photonuclease activity and in vitro antimicrobial efficacy. Spectrochimica Acta Part A: *Molecular and Biomolecular Spectroscopy* 79: 873-883.

Salga MS, Ali HM, Abdulla MA and Abdelwahab SI (2012). Gastroprotective activity and mechanism of novel dichlorido-zinc(II)-4-(2-(5-methoxybenzylideneamino)ethyl)piperazin-1-iumphenolate complex on ethanol-induced gastric ulceration. *Chemico-Biological Interactions* 195: 144-153.

Shahabadi N, Kashanian S and Darabi F (2010). DNA binding and DNA cleavage studies of a water soluble cobalt(II) complex containing dinitrogen Schiff base ligand: The effect of metal on the mode of binding. *European Journal of Medicinal Chemistry* 45: 4239-4245.

Shakir M, Azam M, Ullah MF and Hadi SM (2011). Synthesis, spectroscopic and electrochemical studies of N,N-bis[(E)-2-thienylmethylidene]-1,8-naphthalenediamine and its Cu(II) complex: DNA cleavage and generation of superoxide anion. *Journal of Photochemistry and Photobiology B*: *Biology* 104: 449-456.

Shazia R. Muhammad I. Anwar . Akbar H and Athar A (2010). Transition metal complexes as potential therapeutic agents. *Biotechnology and Molecular Biology Re*views 5: 38-45.

Summerton JE (2007). Morpholino, siRNA, and S-DNA compared: impact of structure and mechanism of action on off-target effects and sequence specificity. *Current Topics in Medicinal Chemistry* 7: 651-60.

Sheldrick GM (2008). A short history of SHELX. Acta Crystallographica Section A A64: 112–122.

Thompson K.H. and Orvig C (2006) . Metal Compounds in Medicinal Chemistry: New Vistas and Challenges in Drug Design. *Dalton Transactions*: 761-764.

Vaidyanathan VG and Nair BU (2003). Photooxidation of DNA by a cobalt(II) tridentate complex. *Journal of Inorganic Biochemistry* 94: 121-126.

Wallace AC, Laskowski RA and JM. T: LIGPLOT (1995). a program to generate schematic diagrams of protein-ligand interactions. *Protein Engineering* 8: 127–134.

Walters J, Pop C, Scott FL, Drag M, Swartz P, Mattos C, Salvesen GS and AC. C (2009). A constitutively active and uninhibitable caspase-3 zymogen efficiently induces apoptosis. *Biochemical Journal* 424: 335-345.

Wang M-Z, Meng Z-X, Liu B-L, Cai G-L, Zhang C-L and Wang X-Y (2005). Novel tumor chemotherapeutic agents and tumor radio-imaging agents: Potential tumor pharmaceuticals of ternary copper(II) complexes. *Inorganic Chemistry Communications* 8: 368-371.

Weiqin Lu, Marcia A. Ogasawara and Huang1 P (2007). Models of reactive oxygen species in cancer. Drug Discovery Today: *Disease Models* 4: 67–73.

Yusnita J, Puvaneswary S, Mohd. Ali H, Robinson WT and Kwai-Lin T (2009). Synthesis, structural characterization and antibacterial activity of 2,6-diacetylpyridine bis(benzenesulfonohydrazide) Schiff bases and their copper(II) complexes. *Polyhedron* 28: 3050-3054.

Zhang Q.L., Liu J.H., Ren X.Z., Xu H., Huang Y., Liu J.Z. and Ji L.N (2003). A functionalized Cobalt(III) mixed-polypyridyl compound as a newly designed DNA molecular light switch. *Journal of Inorganic Biochemistry* 95: 194-102.